07.2

Focused ion beam milling of ridge waveguides of edge-emitting semiconductor lasers

© A.S. Payusov[1], M.I. Mitrofanov[1,2], G.O. Kornyshov[3], A.A. Serin[1], G.V. Voznyuk[1], M.M. Kulagina[1], V.P. Evtikhiev[1], N.Yu. Gordeev[1], M.V. Maximov[3], S. Breuer[4]

[1] Ioffe Institute, St. Petersburg, Russia
[2] Submicron Heterostructures for Microelectronics, Research and Engineering Center, Russian Academy of Sciences, St. Petersburg, Russia
[3] Alferov Federal State Budgetary Institution of Higher Education and Science Saint Petersburg National Research Academic University of the Russian Academy of Sciences, St. Petersburg, Russia
[4] Institute of Applied Physics, Technische University Darmstadt, Darmstadt, Germany
E-mail: plusov@mail.ioffe.ru

Received July 28, 2021
Revised September 12, 2021
Accepted September 28, 2021

We studied the influence of the focused ion beam milling of ridge waveguides on lasing parameters of edge-emitting lasers, based on a separate confinement double heterostructure. It is shown that there are three degrees of influence, according to the etching depth: modification of the waveguide properties only, a decrease in efficiency without changing the threshold current, and a simultaneous deterioration in the threshold current and efficiency with significant modification of the optical characteristics of the laser.

Keywords: focused ion beam, semiconductor laser, optical waveguide, single mode lasing.

DOI: 10.21883/TPL.2022.15.54275.18980

The ridge waveguides of the edge-emitting semiconductor lasers are formed in the course of post-growth processing of laser wafers and determine the basic characteristics of the devices, such as beam quality, the brightness, the maximum power. The latter increases with increasing width of the waveguide. At the same time, however, conditions for the appearance of high-order optical modes arise, and multi-mode lasing becomes possible. This in turn leads to a decrease in the beam quality and brightness. Various approaches have been proposed to maximize the power of edge-emitting lasers operating in the spatially single-mode mode regime: the use of distributed Bragg reflectors and an expanding waveguide [1], the use of gratings built into the waveguide (distributed feedback lasers) [2], the use of modified mirrors [3], local modulation of the effective refractive index [4]. All of them were based on the introduction of elements for spatial and/or spectral selection of optical modes into the waveguide or output mirror. The practical implementation of most of the proposed approaches complicates the manufacture of devices, especially at the stage of creating test samples. When developing a new design of semiconductor lasers using standard post-growth processing techniques, it is necessary to manufacture several devices of the same design that differ in the parameters of the filtering elements in the waveguide, as well as reference samples. This leads to extra time and resource expenses. When investigating the influence of the device design on the parameters of the output beam, especially at the stage of producing test samples, it is convenient to use an off-the-shelf device with a conventional waveguide and make changes to it. The method of direct lithography with a focused ion beam (FIB) is well suited for dealing with tasks of this sort. It allows forming a lithographic pattern in both metal and semiconductor structures with nanometer scale resolution without the use of masks. FIB is widely used in the semiconductor industry and in the laboratories of research groups for the sample preparation for transmission electron microscopes and probes preparation for atomic force microscopes (AFM), as well as modifications of integrated circuits, image sensors, etc. [5]. Recently, it have been used to create nanocavities in optical fibers [6] and to modify mirrors of edge-emitting semiconductor lasers [3]. The disadvantage of the technique is the formation of radiation defects (vacancies, interstitial atoms and their complexes) in the semiconductor structure under the action of high-energy ions. Radiation defects create deep levels in the band gap of the semiconductor, which leads to a decrease in the internal quantum efficiency [7]. According to [7], the formation depth of radiation defects exceeds theoretical estimates by an order of magnitude and reaches $0.85\,\mu$m when etching GaAs/AlGaAs heterostructures with Ga^+ ions with an energy of 30 keV.

The first experiments on waveguide etching of double heterostructure (DHS) lasers have shown that even with a small FIB exposure area of $1\,\mu m^2$ it is possible to dramatically change the lasing spectrum [8]. The carriers in a separate-confinement heterostructures (SC DHS) are localized in the quantum-dimensional active region, this will likely allow one to carry out etching of a larger area and changing the optical properties of the waveguide and laser cavity without affecting recombination in the active

region. However, there are no systematic data on etching of ridge waveguides of SC DHS lasers in the literature. In this work, we studied the dependence of the main optical characteristics of diode lasers with a narrow ridge waveguide on the parameters of their etching by a focused ion beam (the size and depth of the etched region) in order to determine the depth range that make it possible to independently change the optical and electrical properties.

Lasers with ridge width $W = 4\,\mu$m were selected for experiments. The laser wafer was grown by metal-organic vapor phase epitaxy. The active region consists of four layers of quantum well-dots $In_{0.4}Ga_{0.6}As$ [9], separated by GaAs layers with a thickness of 40 nm, and placed in the middle of a GaAs waveguide with a thickness of 450 nm. The thickness of the *p*-cladding with a contact layer is $1.15\,\mu$m, and the *n*-cladding is $1.45\,\mu$m. The ridge waveguides were formed by plasma etching. A contact metal layer Ag/Mn/Ni/Au with a width of $2\,\mu$m and a thickness of 300 nm was deposited on the top of the ridge, then the surface of the structure outside the ridge waveguide was covered with a dielectric layer Si_3N_4 having a thickness of 100 nm, after that the entire surface was covered with Cr/Au metal contact with a thickness of 200 nm. Therefore the surface of the ridge is not planar and has a relief due to the overlap of various layers (Fig. 1, *a*). Samples with a cavity length of $L = 1.5$ mm were mounted on copper heat sinks using indium solder. All laser parameters were measured in pulsed regime with pulse duration of 350 ns and frequency of 3 kHz. Prior to the FIB etching the threshold current density was 530–650 A/cm^2, and differential quantum efficiency (DQE) was a little more than 50%. The lasing wavelength $1.09\,\mu$m corresponds to the ground state of the quantum well-points. Studies of far-fields have shown the multi-mode lasing in the lateral direction.

Etching of the ridge waveguides was carried out in an ultrahigh vacuum by a focused ion beam Ga^+ with an energy of 30 keV and an operating current of 500 pA. The width of the etching area located at $500\,\mu$m from one of the laser mirrors was equal to the width of the waveguide and was $4\,\mu$m, and the length (L_{fib}) for various samples was either $10\,\mu$m, or $50\,\mu$m. This relatively small lengths of the etched region are already sufficient to influence the optical properties of the waveguide [4]. The actual etching depth was determined with AFM images obtained in tapping mode. All heights given below were calculated relative to the interface between the waveguide and the *p*-cladding layers (Fig. 1, *b*). Due to the fact that the contact surface at the top of the ridge was not uniform in height, etching was carried out in two stages. At the first stage, the thickness of the metal contact at the top of the ridge was leveled, at the second — the remaining metal contact and the ridge itself were etched off. Fig. 1, *b* shows the roughness of the bottom of the etched area. It is caused by the rough surface of the metal contact and the influence of the inclined walls of the ridge waveguide on the etching rate and profile. Therefore, in our analysis we used the average height (h_e) and the minimum height ($h_{\min}$) as shown in Fig. 1, *a*. Significant

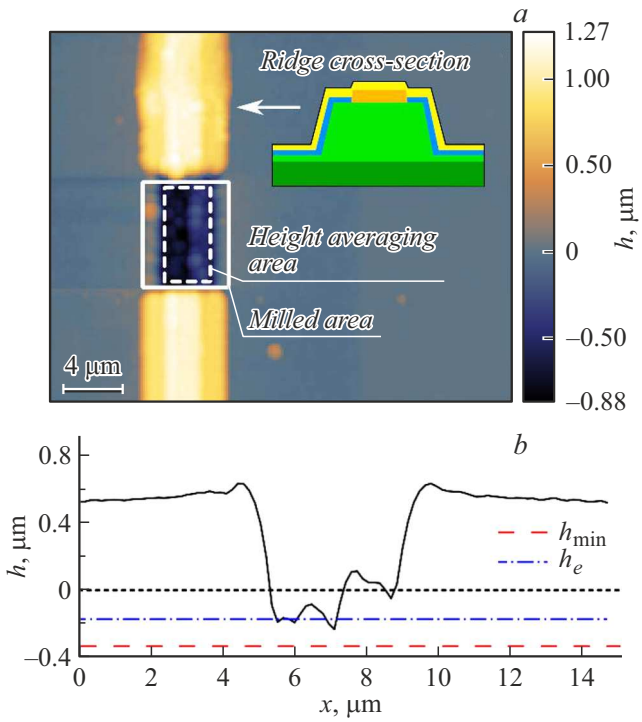

Figure 1. *a* — AFM image of the sample #4. All heights are given relative to the surface of the metal contact between the ridges. The etching area (solid rectangle) and the area in which the average height of h_e (dashed rectangle) was calculated are shown. The insert in the upper right corner shows a schematic profile of the ridge waveguide. *b* — height profile across the waveguide in the middle of the etching area. Zero height corresponds to the interface between waveguide and *p*-cladding layers.

discrepancy between h_e and $h_{\min}$ is associated with the slope of the side walls of the waveguide.

The parameters of laser diodes deteriorate along with an increase in the etching depth, (see table). The probability of forming the radiation defects in active region increases as the etching front approaches to it, which leads to a decrease in internal quantum efficiency and to an increase in the threshold current density I_{th}, accordingly. Therefore, the threshold current density is more affected by the minimum height $h_{\min}$. At the same time, with a small etching depth, an increase in the length of the region by 5 times does not lead to an increase in the threshold current. The change in the differential efficiency of η_D is due to a change in the waveguide parameters. The optical loss associated with scattering in the altered part of the waveguide increase with the increase in the length of the etching region. Thus, it is possible to make changes in the waveguide without increasing the threshold current density by stopping the etching in the *p*-cladding 200–300 nm prior to the the active region layers.

As the depth of etching increased, the lasing spectra shifted to the short wavelength region (Fig. 2) due to the increase of internal losses. Another change in the optical properties of the waveguide, observed already at a minimum

Etching parameters and the relative changes of main characteristics of the devices

Sample number	L_{fib}, μm	Ion dose, 10^{17} cm^{-2}	h_e, μm	$h_{\min}$, μm	I_{th_fib}/I_{th}	η_D/η_{D_fib}
1	10	1.68	+1.4	+0.84	1	1
2	50	1.76	+0.66	+0.21	1	1.55
3	50	1.76	+0.71	+0.08	1	2.07
4	10	7.02	−0.17	−0.33	1.42	3.57
5	10	7.02	+0.08	−0.43	1.53	2.55
6	10	9.78	−0.25	−0.73	1.61	3.33

Note. I_{th_fib} and η_{D_fib}— threshold current and differential efficiency after etching of the FIP, respectively.

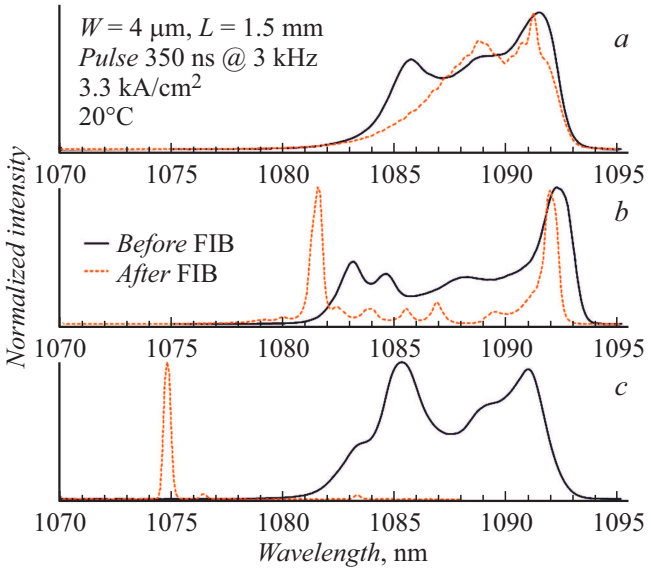

Figure 2. Lasing spectra samples #1 (*a*), #3 (*b*) and #6 (*c*) before and after etching with FIB.

depth of etching is narrowing of lasing spectra. We believe that in this case the etched section works similarly to the passive mode filter [10].

With further increase of the etching depth, the contrast of the effective refractive index along the waveguide becomes sufficient for the laser cavity to split into two optically coupled cavities. Such systems have been studied previously [11,12], and they tend to demonstrate single-frequency lasing, reduced temperature induced shift of the lasing wavelength, and wavelength hopping due to switching from one longitudinal mode to another. The temperature dependencies of the lasing spectra of samples #5 and #6 are typical for lasers with longitudinally coupled cavities (Fig. 3). For these lasers, the temperature shift of the wavelength is determined by the resonance of the longitudinal modes of two coupled cavities and is 0.19 nm/°C. The temperature dependence of the lasing wavelength before etching was determined by the temperature dependence of the energy gap width, and the temperature shift was 0.35 nm/°C. When lasing switched from one hybrid longitudinal mode to another the wavelength changed by 9 nm. The presence of several lasing lines in the spectrum is due to the operation on several lateral modes. This was confirmed by the measurement of far-field patterns.

In conclusion, we have studied the effect of FIB etching of ridge waveguides of edge-emitting semiconductor lasers on their characteristics. It was shown that three ranges of etching depth can be distinguished according to the degree of influence on the laser parameters. When etching stops more than 400 nm prior to the active region, the threshold current density and DQE remain virtually unchanged and do not depend on the etching area, provided that it is relatively small. In this depth range the properties of the laser waveguide and cavity change, and the nature of the changes depends on the size and location of the etched area. Increasing the etching depth to distances of about 200 nm to the active region virtually does not affect the threshold current, but reduces the DQE. In this etching range, the laser cavity starts to split into two optically coupled cavities. The increase of the threshold current during FIB etching begins at a greater depth, when radiation defects begin to form in the active region. The results of our study can be used both to create high-power spatially single-mode laser diodes

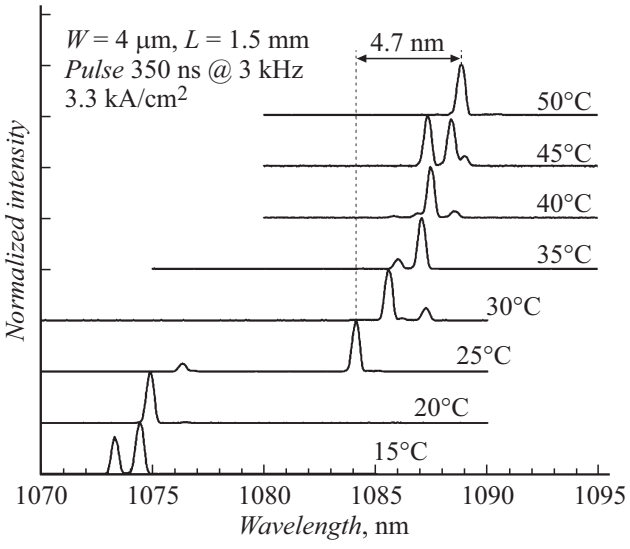

Figure 3. Temperature dependence of the lasing spectra of the sample #6 after FIB etching.

and to improve the beam quality in the lateral direction of high-power broad area lasers [13].

Acknowledgment

The research was funded by the Ministry of High Education and Science of the Russian Federation under the project 0791-2020-0002, and by the Russian Foundation for Basic Research under projects 19-32-90219 and 18-502-12081. S. Breuer acknowledges the support from the German Research Foundation (DFG) (project N 389193326).

Conflict of interest

The authors declare that they have no conflict of interest.

References

[1] K. Paschke, F. Bugge, G. Blume, D. Feise, G. Erbert, Opt. Lett., **40**, 100 (2015). DOI: 10.1364/OL.40.000100
[2] H. Wenzel, A. Klehr, M. Braun, F. Bugge, G. Erbert, J. Fricke, A. Knauer, P. Ressel, B. Sumpf, M. Weyers, G. Traenkle, Proc. SPIE, **5594**, 110 (2004). DOI: 10.1117/12.569039
[3] N.Yu. Gordeev, A.S. Payusov, I.S. Mukhin, A.A. Serin, M.M. Kulagina, Yu.A. Guseva, Yu.M. Shernyakov, Yu.M. Zadiranov, M.V. Maximov, Semiconductors, **53**, 200 (2019). DOI: 10.1134/S1063782619020106.
[4] S. O'Brien, A. Amann, R. Fehse, S. Osborne, E.P. O'Reilly, J.M. Rondinelli, J. Opt. Soc. Am. B, **23**, 1046 (2006). DOI: 10.1364/JOSAB.23.001046
[5] R.M. Langford, A.K. Petford-Long, M. Rommeswinkle, S. Egelkamp, Mater. Sci. Technol., **18**, 743 (2002). DOI: 10.1179/026708302225003893
[6] P. Romagnoli, M. Maeda, J.M. Ward, V.G. Truong, S.N. Chormaic, Appl. Phys. B, **126**, 111 (2020). DOI: 10.1007/s00340-020-07456-x
[7] G.V. Voznyuk, I.N. Grigorenko, M.I. Mitrofanov, D.N. Nikolaev, M.N. Mizerov, V.P. Evtikhiev, Semoconductors, **54**, 1869 (2020). DOI: 10.1134/S1063782620140316
[8] C.R. Musil, B.D. Patterson, H. Auderset, Nucl. Instrum. Meth. Phys. Res. B, **127-128**, 428 (1997). DOI: 10.1016/S0168-583X(96)00968-8
[9] M.V. Maximov, A.M. Nadtochiy, S.A. Mintairov, N.A. Kalyuzhnyy, N.V. Kryzhanovskaya, E.I. Moiseev, N.Yu. Gordeev, Yu.M. Shernyakov, A.S. Payusov, F.I. Zubov, V.N. Nevedomskiy, S.S. Rouvimov, A.E. Zhukov, Appl. Sci., **10**, 1038 (2020). DOI: 10.3390/app10031038
[10] N.Yu. Gordeev, I.I. Novikov, A.M. Kuznetsov, Yu.M. Shernyakov, M.V. Maximov, A.E. Zhukov, A.V. Chunareva, A.S. Payusov, D.A. Livshits, A.R. Kovsh, Semiconductors, **44**, 1357 (2010). DOI: 10.1134/S1063782610100192.
[11] H. Temkin, J.P. van der Ziel, R.A. Linke, R.A. Logan, Appl. Phys. Lett., **43**, 723 (1983). DOI: 10.1063/1.94490
[12] D. Marcuse, T.-P. Lee, IEEE J. Quantum Electron., **20**, 166 (1984). DOI: 10.1109/JQE.1984.1072360
[13] J. Rong, E. Xing, L. Wang, S. Shu, S. Tian, C. Tong, L. Wang, Appl. Phys. Express, **9**, 072104 (2016). DOI: 10.7567/APEX.9.072104